Polarized synchrotron radiation as a tool for studying runaway electrons

M. Hoppe[1], R. A. Tinguely[2], B. Brandström[1], O. Embreus[1], N. C. Hawkes[3], E. Rachlew[1], T. Fülöp[1] and JET contributors*

[1]Department of Physics, Chalmers University of Technology, SE-41296 Gothenburg, Sweden
[2]Plasma Science and Fusion Center, Massachusetts Institute of Technology, Cambridge, MA 02139, USA
[3]UKAEA-CCFE, Culham Science Centre, Abingdon, Oxon OX14 3DB, United Kingdom
*See the author list of '*Overview of JET results for optimising ITER operation*' by J. Mailloux et al. to be published in *Nuclear Fusion Special issue: Overview and Summary Papers* from the 28th Fusion Energy Conference (Nice, France, 10-15 May 2021)

CHALMERS

Email:
hoppe@chalmers.se

PSFC

Summary

Synchrotron radiation can be used to diagnose relativistic runaway electrons, typically by measuring the radiation spectrum or recording camera images. Recently, the Alcator C-Mod Motional Stark Effect (MSE) diagnostic was used to also measure the polarization of synchrotron radiation [1]. In this contribution we use the SOFT synthetic synchrotron diagnostic framework [2] to simulate the response of the Joint European Torus (JET) MSE diagnostic [3] to synchrotron radiation from runaway electrons with different energies and pitch angles. In particular, we study the linear polarization fraction $f_{\rm pol}$ and polarization angle $\theta_{\rm pol}$.

We find that a threshold in pitch angle exists in both the polarization fraction and angle. At the threshold, the polarization fraction goes to zero while the polarization angle transitions from $\theta_{\rm pol}=0^\circ$ to $\theta_{\rm pol}=90^\circ$. This threshold was also observed in Alcator C-Mod [1] and was proposed as a useful indicator for constraining the pitch angle of the electrons dominating synchrotron emission. In the magnetic geometry of the particular JET discharge considered here, #94508, the threshold occurs at a very small pitch angle, and does not vary appreciably between MSE diagnostic channels. Therefore, the threshold could likely not be used to constrain the pitch angle in this particular magnetic geometry. It might however be possible to constrain the pitch angle in other pulses, particularly if the plasma is more vertically offset relative to the MSE diagnostic.

JET MSE geometry

The JET MSE diagnostic consists of 25 channels viewing the plasma tangentially. Each channel receives most of its light from a narrow range of flux surfaces. Here, we consider the magnetic geometry of JET pulse #94508 at t = 48.5s, reconstructed with EFIT [8] and shown to the right. The blue crosses indicate the points where the diagnostic lines-of-sight are tangential to the plasma. The figure on the bottom-left gives the diagnostic sensitivity as a function of radius for each channel. Due to the vertical offset of the plasma, the diagnostic cannot view the plasma centre.

Flux surfaces (black contours) and lines-of-sight (blue crosses) in #94508 at t = 48.5s.

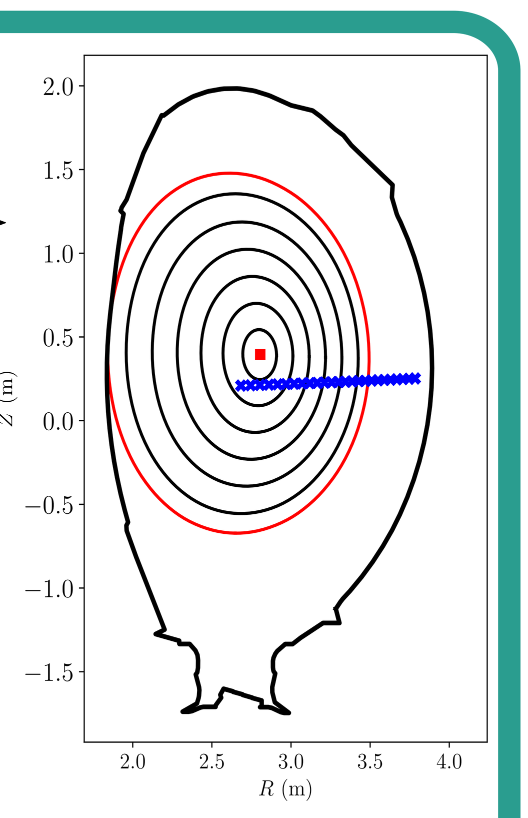

Sensitivity of the 25 MSE diagnostic channels to radiation from different flux surfaces in #94508.

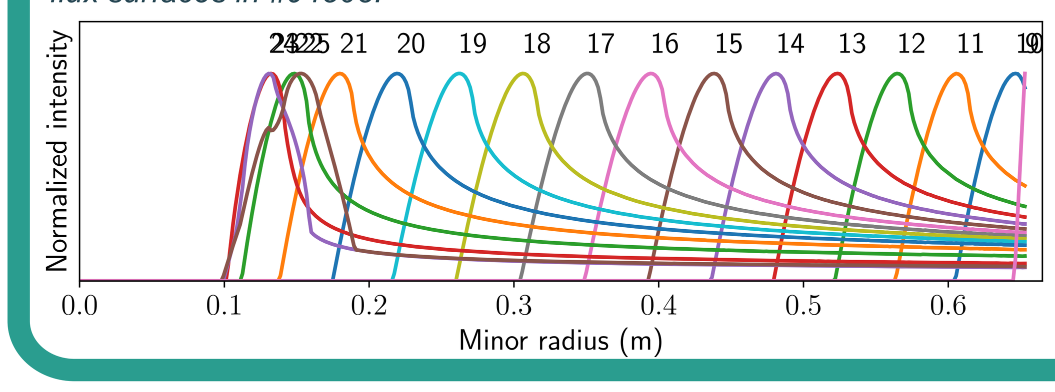

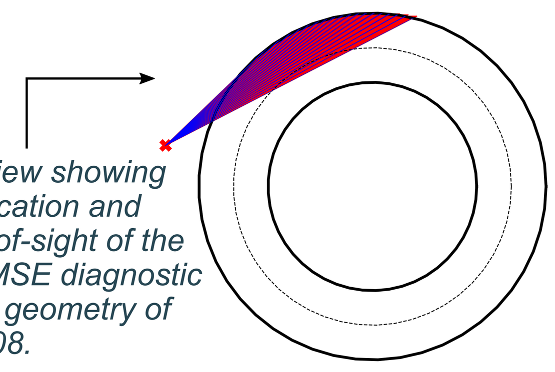

Top view showing the location and lines-of-sight of the JET MSE diagnostic in the geometry of #94508.

SOFT Green's functions

SOFT [2] calculates the radiation power received by an observer. The radiation power can be cast on the form

$$P=\int G(R,p,\theta_{\rm p})f(R,p,\theta_{\rm p})\,p^2\sin\theta_{\rm p}\,{\rm d}R\,{\rm d}p\,{\rm d}\theta_{\rm p}$$

where $f(R,p,\theta_{\rm p})$ is the electron distribution function, and $G(R,p,\theta_{\rm p})$ is the diagnostic Green's function which describes the diagnostic signal due to electrons on the flux surface labeled by R, with momentum p and pitch angle $\theta_{\rm p}$ in the point of minimum magnetic field along the orbit.

Polarization filter model

The irradiance behind a linear polarizer in the setup illustrated in the figure below can be given in terms of Stokes parameters [5]:

$$\mathcal{I}(\psi)=\frac{1}{2}\left(I+Q\cos 2\psi+U\sin 2\psi\right)$$

By making measurements at $\psi=0$, $\psi=\pi/4$ and $\psi=\pi/2$ we can then solve for the Stokes parameters

$$I=\mathcal{I}(0)+\mathcal{I}(\pi/2),$$
$$Q=\mathcal{I}(0)-\mathcal{I}(\pi/2),$$
$$U=2\mathcal{I}(\pi/4)-\mathcal{I}(0)-\mathcal{I}(\pi/2).$$

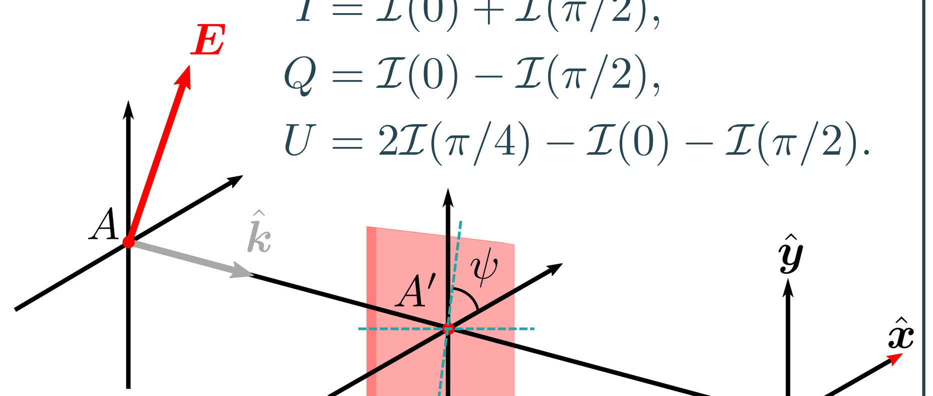

Stokes V vanishes identically for synchrotron radiation [4] and is hence not considered here. This is equivalent to saying that synchrotron radiation is not circularly polarized.

When the light propagation vector $\hat{\boldsymbol{k}}$ is ***not*** perpendicular to the polarizer plane, we consider the model proposed in [6]. There, the polarizer is assumed to absorb light which is polarized along the axis $\hat{\boldsymbol{a}}=\hat{\boldsymbol{y}}\cos\psi-\hat{\boldsymbol{x}}\sin\psi$, and allow any other polarization component to be transmitted. For arbitrary $\hat{\boldsymbol{k}}$, light is assumed to be absorbed along the *effective absorption axis*

$$\hat{\boldsymbol{a}}_{\rm eff}=\frac{\hat{\boldsymbol{a}}-\hat{\boldsymbol{k}}\left(\hat{\boldsymbol{a}}\cdot\hat{\boldsymbol{k}}\right)}{\sqrt{1-\left(\hat{\boldsymbol{a}}\cdot\hat{\boldsymbol{k}}\right)^2}}\quad\Longrightarrow\quad \begin{array}{l}\mathcal{I}=\epsilon_0 c|T_{\rm p}\boldsymbol{E}|^2\\ T_{\rm p}=\mathbb{I}-\hat{\boldsymbol{a}}_{\rm eff}\hat{\boldsymbol{a}}_{\rm eff}\end{array}$$

The irradiance is then given by $\mathcal{I}(\psi)=\epsilon_0 c|\boldsymbol{E}-\hat{\boldsymbol{a}}_{\rm eff}\left(\hat{\boldsymbol{a}}_{\rm eff}\cdot\boldsymbol{E}\right)|^2$. By decomposing $\boldsymbol{E}$ as [7], $\boldsymbol{E}=\hat{\boldsymbol{e}}_\perp E_\perp-i\hat{\boldsymbol{e}}_\parallel E_\parallel$, where $\hat{\boldsymbol{e}}_\parallel$ is a unit vector in the direction of acceleration, and $\hat{\boldsymbol{e}}_\perp$ a unit vector in the plane perpendicular to $\hat{\boldsymbol{e}}_\parallel$, we can express the irradiances needed to evaluate the Stokes parameters to the left as

$$\mathcal{I}(0)=\frac{E_\perp^2\left(\hat{\boldsymbol{y}}\cdot\hat{\boldsymbol{e}}_\parallel\right)^2+E_\parallel^2\left(\hat{\boldsymbol{y}}\cdot\hat{\boldsymbol{e}}_\perp\right)^2}{\left(\hat{\boldsymbol{y}}\cdot\hat{\boldsymbol{e}}_\parallel\right)^2+\left(\hat{\boldsymbol{y}}\cdot\hat{\boldsymbol{e}}_\perp\right)^2},\quad \mathcal{I}(\pi/2)=\frac{E_\perp^2\left(\hat{\boldsymbol{x}}\cdot\hat{\boldsymbol{e}}_\parallel\right)^2+E_\parallel^2\left(\hat{\boldsymbol{x}}\cdot\hat{\boldsymbol{e}}_\perp\right)^2}{\left(\hat{\boldsymbol{x}}\cdot\hat{\boldsymbol{e}}_\parallel\right)^2+\left(\hat{\boldsymbol{x}}\cdot\hat{\boldsymbol{e}}_\perp\right)^2}$$

$$\mathcal{I}(\pi/4)\quad\frac{E_\perp^2\left(\hat{\boldsymbol{x}}\cdot\hat{\boldsymbol{e}}_\parallel-\hat{\boldsymbol{y}}\cdot\hat{\boldsymbol{e}}_\parallel\right)^2+E_\parallel^2\left(\hat{\boldsymbol{x}}\cdot\hat{\boldsymbol{e}}_\perp-\hat{\boldsymbol{y}}\cdot\hat{\boldsymbol{e}}_\perp\right)^2}{\left(\hat{\boldsymbol{x}}\cdot\hat{\boldsymbol{e}}_\parallel-\hat{\boldsymbol{y}}\cdot\hat{\boldsymbol{e}}_\parallel\right)^2+\left(\hat{\boldsymbol{x}}\cdot\hat{\boldsymbol{e}}_\perp-\hat{\boldsymbol{y}}\cdot\hat{\boldsymbol{e}}_\perp\right)^2}$$

Polarization fraction

The linear polarization fraction $f_{\rm pol}$ is defined in terms of the Stokes parameters as

$$f_{\rm pol}=\frac{\sqrt{Q^2+U^2}}{I}$$

SOFT Green's functions for the linear polarization fraction measured by a few MSE diagnostic channels are shown below. The polarization fraction depends weakly on momentum p, but shows more structure as a function of pitch angle $\theta_{\rm p}$. The gray regions in the figure below indicate regions of no radiation received. A threshold in pitch angle appears in all MSE diagnostic channels at small pitch angle. Around the threshold, the polarization fraction goes to zero. The reason for the threshold is illustrated in the right figure, which shows synchrotron camera images, coloured according to the linear polarization fraction in each pixel, and overlaid with green circles indicating the MSE diagnostic lines-of-sight. Near the edges of the synchrotron spot, the polarization fraction goes to zero. Since the lines-of-sight are vertically aligned fairly close to the centre of the synchrotron spot in #94508, $f_{\rm pol}=0$ will only be recorded when the synchrotron spot is sufficiently contracted, which only occurs at small pitch angles. Since the threshold varies little with MSE channel, it can likely not be used to constrain the pitch angle of the dominant particles in #94508. It might however be possible to utilize it in other pulses, where the plasma is more vertically offset.

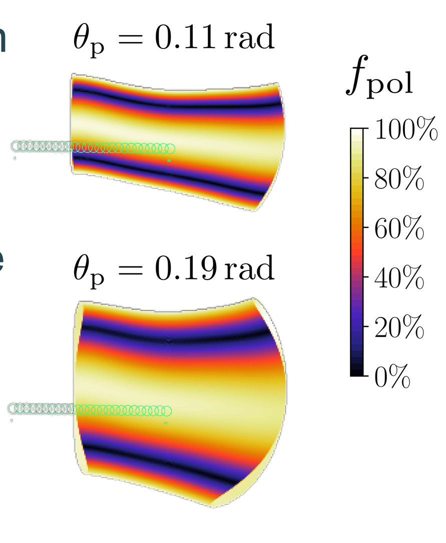

Synchrotron camera images, coloured according to the polarization fraction received

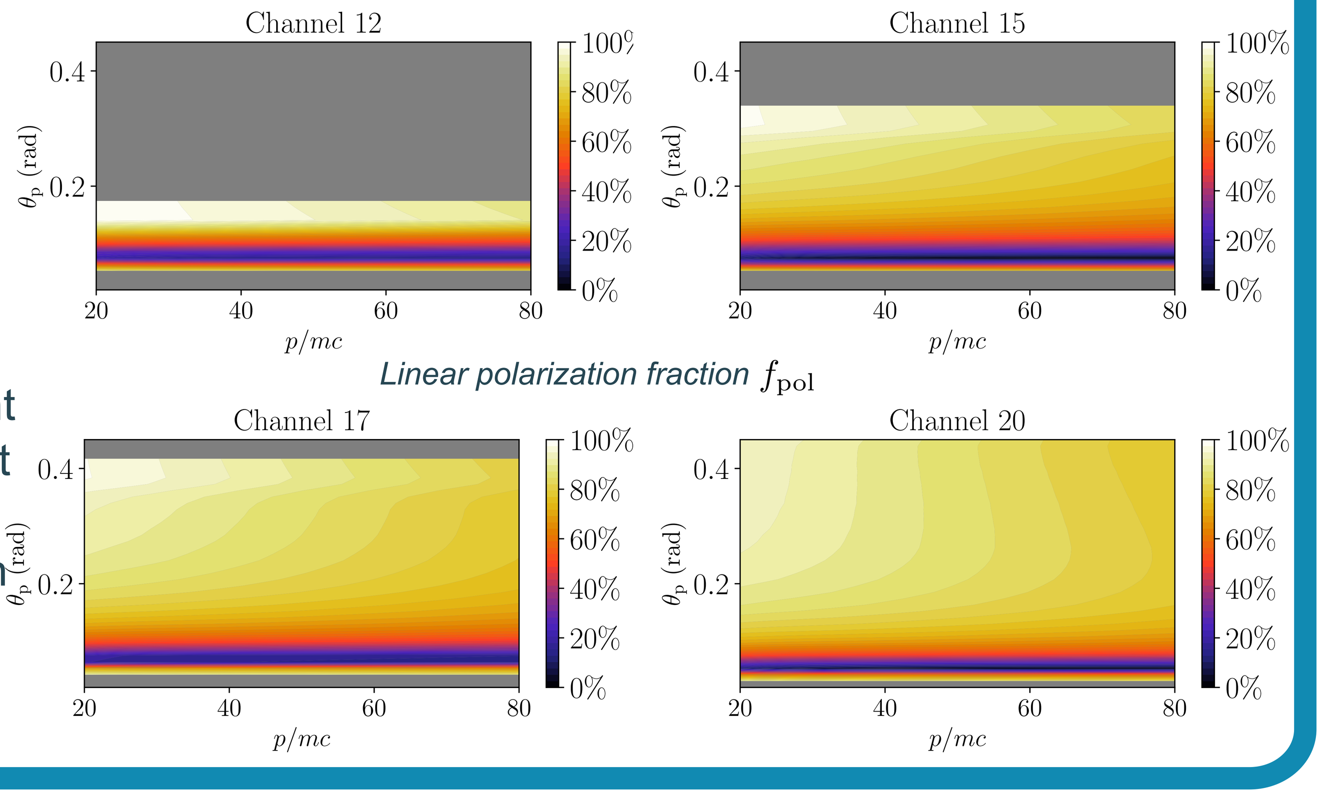

Linear polarization fraction $f_{\rm pol}$

Polarization angle

The polarization angle is defined in terms of the Stokes parameters as

$$\theta_{\rm pol}=\frac{1}{2}\arctan\frac{U}{Q}$$

The figure below shows the polarization angle as measured by four MSE diagnostic channels as functions of momentum p and pitch angle $\theta_{\rm p}$. As with the polarization fraction, a threshold is found in all channels at a small pitch angle where the polarization angle transitions from $\theta_{\rm pol}=0^\circ$ to $\theta_{\rm pol}=90^\circ$. This threshold was first pointed out in [1] for Alcator C-Mod. Similar to the polarization fraction, the threshold occurs because the polarization near the upper and lower edges of the synchrotron spot (shown in the right figure of the polarization fraction section) becomes $\theta_{\rm pol}=0^\circ$. Because of the small value of the threshold, and slow variation with MSE channel number, the threshold cannot be used to constrain the pitch angle of the dominant emitting particles in #94508. It might however be used in other pulses where the plasma is more vertically offset relative to the MSE diagnostic.

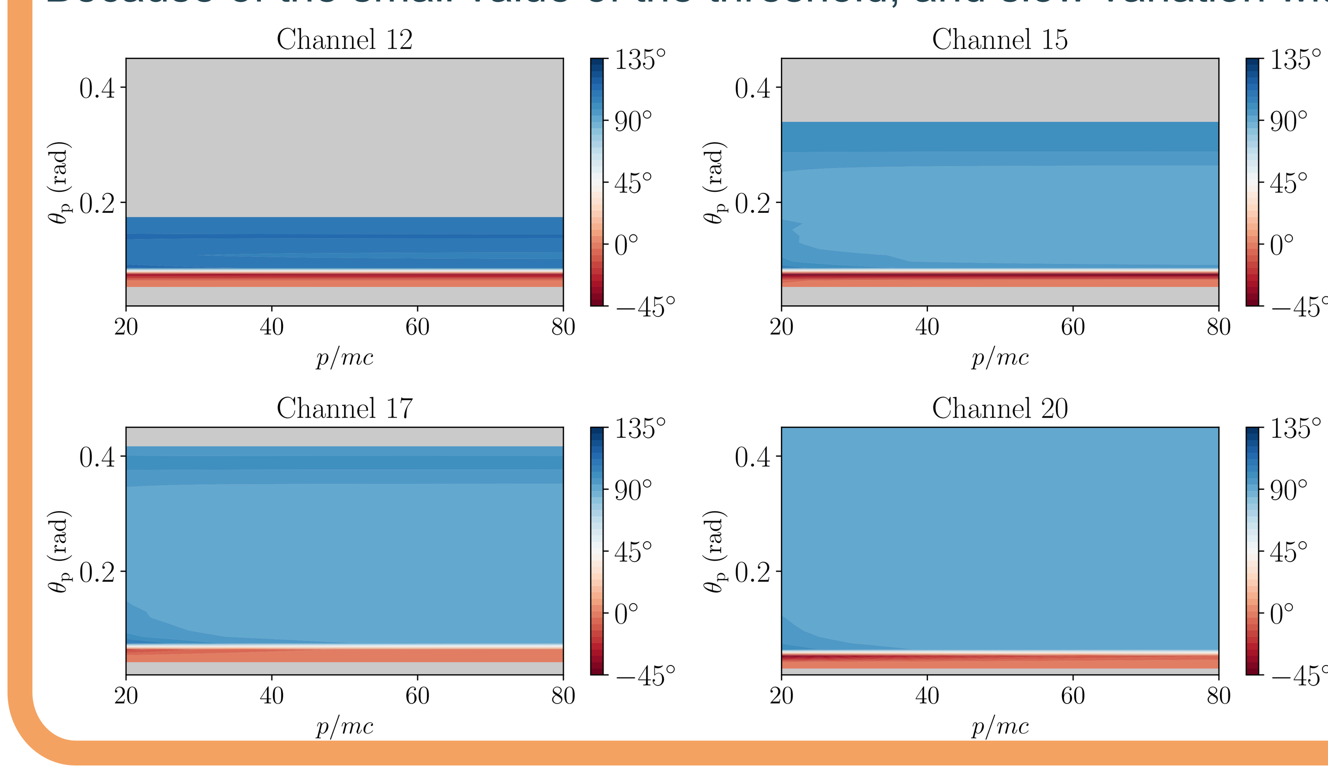

References

[1] R. A. Tinguely *et al.* Nucl. Fusion **59** 096029 (2019).
[2] M. Hoppe *et al.* Nucl. Fusion **58** 026032 (2018).
[3] N. C. Hawkes *et al.* Rev. Sci. Instrum. **70** 894 (1999).
[4] A. A. Korchakov *et al.* SvA **5** 678 (1962).
[5] J. M. Stone, *Radiation and optics*, McGraw-Hill (1963).
[6] J. Korger *et al.* Opt. Express **21** 27032 (2013).
[7] J. D. Jackson, Classical Electrodynamics John Wiley & Sons (1999).
[8] D. P. O'Brien *et al.* Nucl. Fusion **32** 1351 (1992)